Available online at www.sciencedirect.com

ScienceDirect

Journal of the European Ceramic Society 29 (2009) 155–162

www.elsevier.com/locate/jeurceramsoc

Wear behaviour of α- and α/β-SiAlON ceramics stabilized with Nd_2O_3 and Y_2O_3

S. Kurama[a,*], I. Schulz[b], M. Herrmann[c]

[a] Anadolu University, Department of Materials Science and Engineering, 26555 Eskisehir, Turkey
[b] Technical University Dresden, Institute of Material Science, Dresden, Germany
[c] Fraunhofer Institute for Ceramic Technologies and Systems, D-01277, Dresden, Germany

Received 14 February 2008; received in revised form 20 May 2008; accepted 24 May 2008

Abstract

α- and α/β-SiAlON compositions, doped with Y_2O_3 or Nd_2O_3, were densified by gas pressure sintering (GPS). The wear and mechanical properties of the materials were investigated and compared to β-Si_3N_4 materials. Microstructure evolution and its change with composition as well as the influence of the microstructural changes on the mechanical and tribological properties were reported. Wear tests were performed using a tribometer with ball-on-plate geometry in reciprocating sliding contact under dry condition. It was observed that α/β-SiAlON compositions, doped with Y_2O_3, have better wear properties in comparison to α-SiAlON and β-Si_3N_4 samples. Field emission scanning electron microscopy (FESEM) was used to analyse the worn surfaces after wear tests. The results showed that α/β-SiAlON and β-Si_3N_4 materials have different wear behaviour.

Keywords: Grain boundary phase; Wear resistance; SiAlON; Cutting tools; Mechanical properties

1. Introduction

Several structural ceramics are widely used in tribological applications due to their high hardness, elastic modulus and good wear behaviour. Among the non-oxide ceramics, Si_3N_4-based ceramics were intensively investigated over the last decades for several potential engineering applications because of their superior combination of properties,[1] such as retention of high strength over a wide range of temperature as well as high toughness and hardness. SiAlON ceramics are closely related to silicon nitride. They are solid solutions where the Si and N elements are replaced by Al or O. α- and β-SiAlON are isostructural with α- and β-Si_3N_4. β-SiAlON has the formula $Si_{6-z}Al_zO_zN_{8-z}$ where $z \leq 4.0$. α-SiAlON is well established compounds with the general formula $M_xSi_{12-(m+n)}Al_{m+n}O_nN_{16-n}$, where M is one of the cations (Li, Mg, Ca and Y) and most rare earths (excluding La, Ce, Pr and Eu); m is the number of Si–N bonds in α-Si_3N_4 replaced by Al–N; n is the number of Si–N bonds in α-Si_3N_4 replaced by Al–O; and x is equal to m divided by the valency of the M cation.[2] Due to their superior properties they have great potential for many commercial applications requiring wear resistance, high fracture toughness, chemical stability and high temperature stability. Accordingly, this material has potential application in cutting tools, bearing parts, rollers, refractory parts etc. The used oxide sintering aids result in materials containing a significant amount of glassy intergranular boundary phase, typically around 10 wt%. The properties of the materials are therefore determined to a large extent by the properties of this phase. The reduction of the amount of grain boundary is important for tailoring the properties.

In α-SiAlON materials with rare-earth additives the mechanical properties can be adjusted by varying the ratio of α- to β-SiAlON. Additionally, they also provide the possibility to reduce the grain boundary phase because the rare-earth ions can be accommodated in α-SiAlON.[3,4]

It is well known that mechanical, tribological and chemical properties of α- and α/β-SiAlON ceramics are affected by chemical composition, microstructure and crystal structure. The tribological response of SiAlON ceramics as self-mated pairs or as dissimilar couples with metals was investigated in a wide range of experimental conditions like speed, load, temperatures,

---

* Corresponding author. Tel.: +90 222 321 3550x6372; fax: +90 222 323 9501.
E-mail address: skurama@anadolu.edu.tr (S. Kurama).

0955-2219/$ – see front matter © 2008 Elsevier Ltd. All rights reserved.
doi:10.1016/j.jeurceramsoc.2008.05.040

lubrication, and humidity.[5–25] However, only few published papers relate the microstructure grain size and morphology, the amount and nature of intergranular phase as well as the ceramic composition to wear behaviour.[16,17] Therefore, the optimisation of the tribological properties with regard to microstuctural design is still a matter of research.

In this study, various contents of Nd_2O_3 and Y_2O_3 were used as sintering additives for the production of α- and α/β-SiAlON materials. The aim of this study was to investigate the effect of these sintering additives and the influence of the amount of grain boundary phase on the mechanical properties, hardness and fracture toughness of SiAlON ceramics. Friction and wear behaviour of these SiAlON ceramics were also investigated in reciprocating sliding contact under 50% of relative humidity and without lubricants.

2. Experimental

2.1. Material preparation

The starting powders, Si_3N_4 (UBE-10, containing 1.6% oxygen), AlN (Tokuyama, containing 1% oxygen), Al_2O_3 (99.99%, Sumitomo AES IIC), Y_2O_3 and Nd_2O_3 (99.99% H.C. Starck), were mixed as shown in Table 1. The powders were mixed in a planetary ball mill using isopropanol as a solvent. The samples were pressed to bars $20 \times 50 \times 20\,mm^3$ by cold isostatic pressing at 200 MPa. Afterwards, the samples were densified by gas pressure sintering (GPS) at 1825 °C for 90 min. For sintering Y_2O_3 and Nd_2O_3 were chosen as additives due to their different ionic radii and stabilisation behaviour in the α-SiAlON structure. The starting compositions and the designation of the samples are given in Table 1. One of the compositions was selected in the α/β-SiAlON region ($m = 0.5$ and $n = 1.0$). The other composition was selected within the single α-SiAlON region ($m = 1.25$ and $n = 1.0$). 2 wt% excess amounts of additives were also used to show that the amount of sintering additives affects the wear and mechanical properties. In addition, two different Si_3N_4 materials, densified by hot pressing at 1700 and 1850 °C with 11 wt% of amorphous phase (6 wt% Y_2O_3 and 5 wt% Al_2O_3), were selected as reference materials.

2.2. Characterisation

The density of the samples was measured using the Archimedes method. The surface of the sintered samples was removed (at least 4 mm) and then the phase composition was analysed by X-ray diffraction (XRD 7 Seifert, FPM; Cu Kα). Quantitative XRD analysis and the determination of the occupation factors were performed with the software REFINE++ (Seifert FPM).[26] The microstructure was characterised by means of a field emission scanning electron microscope (FESEM, Leo 982, Germany).

Hardness and fracture toughness were measured using a Vickers diamond indenter on a polished surface with a load of 10 kg. K_{IC} values were calculated using the formula[27]:

$$K_{IC} = k\left(\frac{E}{H}\right)^{1/2} \times F \times c^{-3/2} \times 0.0316\,[\mathrm{MPam}^{1/2}]$$

E, Young's modulus (GPa), H, hardness (GPa), F, load (N), c = crack length (μm), k, dimensionless constant (0.016 ± 0.004).

The results are presented as the average of five separate measurements. The initial surface roughness of the samples was characterised after grinding and polishing with 6 μm diamond grains by using stylus profilometry (Hommelwerke-LV-50) with a stylus tip radius of 5 μm (TK E100). Table 2 shows the resulting values of the surface roughness according to the German standard DIN 4762-4287.

Prior to the friction tests all samples were cleaned in an ultrasonic bath with acetone for 5 min, and then dried in hot air. Wear tests were carried out using the SRV III Optimol friction tester (Optimol Instruments GMBH, Germany) in ball-on-disk configurations under sliding conditions with 25 cycles per second and an amplitude of 2 mm. The sliding pair consisted of a ceramic sample ($10 \times 10 \times 10\,mm^3$) and a bearing steel ball (100Cr6, Ø10 mm) which formed the upper oscillating specimen. In comparison, tests were conducted against a silicon nitride ball with Ø10 mm. In order to eliminate the contribution of the lubricant, wear tests were generally conducted under dry conditions in air. Temperature and humidity were kept within 25 ± 3 °C and 50 ± 5% RH, respectively. Sliding conditions were set at a slid-

Table 1
Sample designations and compositions

Sample	m	n	Additive		Excess Nd_2O_3 (2 wt%)	Excess Y_2O_3 (2 wt%)	Density (g/cm^3)	Porosity (%)
			Nd_2O_3	Y_2O_3				
N1251	1.25	1.0	●	–	–	–	3.40	–
N1251-E2	1.25	1.0	●	–	●	–	3.44	–
N051	0.5	1.0	●	–	–	–	2.37	12.47
N051-E2	0.5	1.0	●	–	●	–	3.29	0.05
Y051	0.5	1.0	–	●	–	–	1.98	34.26
Y051-E2	0.5	1.0	–	●	–	●	3.24	0.10
Y1251	1.25	1.0	–	●	–		2.76	2.28
Y1251-E2	1.25	1.0	–	●	–	●	3.31	–
485-Si_3N_4[a]	–	–	–	–	–	–	–	–
480-Si_3N_4[b]	–	–	–	–	–	–	–	–

[a] Sintered at 1850 °C.

[b] Sintered at 1700 °C.

Table 2
Values of the surface roughness parameters, hardness and toughness of SiAlON and for Si_3N_4 materials investigated

Sample	K_{IC} (MPam$^{1/2}$)	HV10 (GPa)	Surface roughness parameter mean values (μm)	
			R_a	R_z
N1251	4.2 ± 0.15	18.9 ± 0.15	0.03	0.29
N1251-E2	4.2 ± 0.40	18.7 ± 0.40	0.035	0.35
N051-E2	4.6 ± 0.24	17.9 ± 0.24	0.03	0.27
Y051-E2	4.8 ± 0.5	18.2 ± 0.5	0.04	0.34
Y1251-E2	3.0 ± 0.4	18.2 ± 0.4	0.04	0.39
485-Si_3N_4	5.8 ± 0.3	15.1 ± 0.3	0.03	0.18
480-Si_3N_4	5.5 ± 0.2	15.8 ± 0.2	0.03	0.19

R_a: arithmetic average surface roughness value; R_z: the arithmetic average values of the sum of the highest and the lowest values.

ing speed of 0.1m/s and a normal load of 10, 20 and 30 N. The sliding time was set at 1 h.

The wear area of the ball and the length of the wear scar on the samples were determined with an optical microscope connected with the soft imaging system AnalySIS. The sectional worn areas of the samples were measured at three points perpendicularly to the sliding direction, using a contact type roughness tester (Hommelwerke-LV-50). The worn volume of the samples (ΔV) was calculated by integration of the sectional worn area. The specific wear rate (w) was calculated by the equation:

$$w = \frac{\Delta V}{Fd} \tag{1}$$

where F [N] and d [m] are normal load and sliding distance.

3. Results

The starting compositions, XRD results, lattice parameters, calculated x values, density and mass change of the samples are summarised in Table 3. The XRD results showed that all materials consist of α- and/or β-SiAlON. No crystalline grain boundary phase was observed. All materials had almost full theoretical density except for the N051 and Y051 samples having a porosity of 12 or 34% (Table 1). These samples (N051 and Y051) were not analysed under tribological, mechanical and microstructural test due to their low density.

Even though Nd- and Y-doped materials with $m = 1.25$ and $n = 1$ showed a single-phase composition the calculated x values of N1251 ($Nd_xSi_{12-(m+n)}Al_{m+n}O_nN_{16-n}$) are slightly lower than the theoretical values. This indicates that a higher amount of a grain boundary phase is formed in the Nd-α-SiAlON materials.

3.1. Friction and wear behaviour

The wear images of the SiAlON materials N1251 (Fig. 1a) and Y051-E2 (Fig. 2a) after fretting tests against a steel ball show that mainly mild tribochemical assisted wear was conducted up to a load of 30 N which corresponds with a maximum Hertzian pressure of 1700 MPa. By contrast, the worn surfaces after fretting tests against a 10 mm silicon nitride ball show heavy wear (Fig. 1b and Fig. 2b) which is characterised by microcracking and removal of grains at a maximum Hertzian pressure of 1700 MPa corresponding with a load of 20 N. These differences are caused by the developed surface layers. In the tribocontact against steel, FeO_x could be detected in addition to SiO_x by EDX at the worn surface (Fig. 3). This special surface layer works as a lubricant tribo layer and can better distribute the contact stress. The friction coefficient and specific wear rate (w) versus load of the investigated SiAlON tribopairs including β-Si_3N_4 reference materials (485 and 480) against the steel ball are given in Figs. 4 and 5. It is obvious that the starting composition and applied loads have important influence on the wear behaviour of

Table 3
Density, mass change and XRD results of the samples

Sample	Theoretical x-values	Phases	Lattice parameters (α-SiAlON)	Calculated x-value	Density (g/cm^3)	Δm (%)
N1251	0.42	α-SiAlON	$a = 7.81737 \pm 0.0005$ $c = 5.69612 \pm 0.0004$	0.36 ± 0.01	3.40	0.47
N1251-E2	0.42	α-SiAlON	$a = 7.83136 \pm 0.0002$ $c = 5.70650 \pm 0.0003$	0.38 ± 0.01	3.44	0.50
N051	–	55.4 ± 0.3 α-SiAlON 44.6 ± 0.3 β-SiAlON	$a = 7.80460 \pm 0.0001$ $c = 5.68213 \pm 0.0002$	0.28 ± 0.01	2.37	0.46
N051-E2	–	74.4 ± 0.4 α-SiAlON 25.6 ± 0.4 β-SiAlON	$a = 7.80319 \pm 0.0004$ $c = 5.68201 \pm 0.0003$	0.26 ± 0.01	3.29	0.51
Y051-E2		81.1 ± 0.3 α-SiAlON 18.9 ± 0.3 β-SiAlON	$a = 7.79803 \pm 0.0001$ $c = 5.67731 \pm 0.0002$	0.25 ± 0.01	3.24	0.54
Y1251-E2	0.42	α-SiAlON	$a = 7.82101 \pm 0.0001$ $c = 5.70008 \pm 0.0002$	0.41 ± 0.01	3.31	0.52

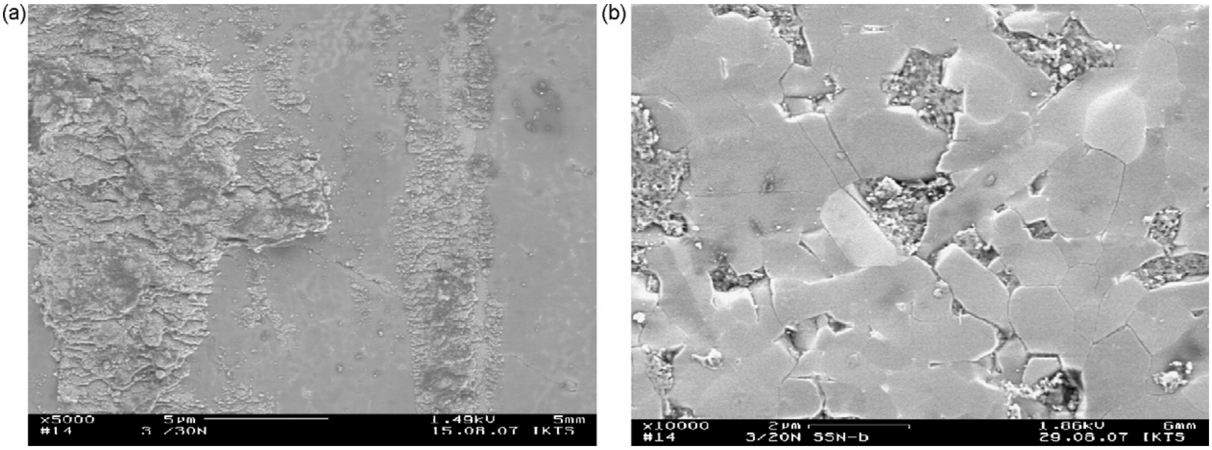

Fig. 1. FESEM micrographs of the worn surfaces of the N1251 material after fretting at a maximum Hertzian pressure of 1700 MPa against a 10 mm ball of (a) steel 100Cr6 and (b) silicon nitride.

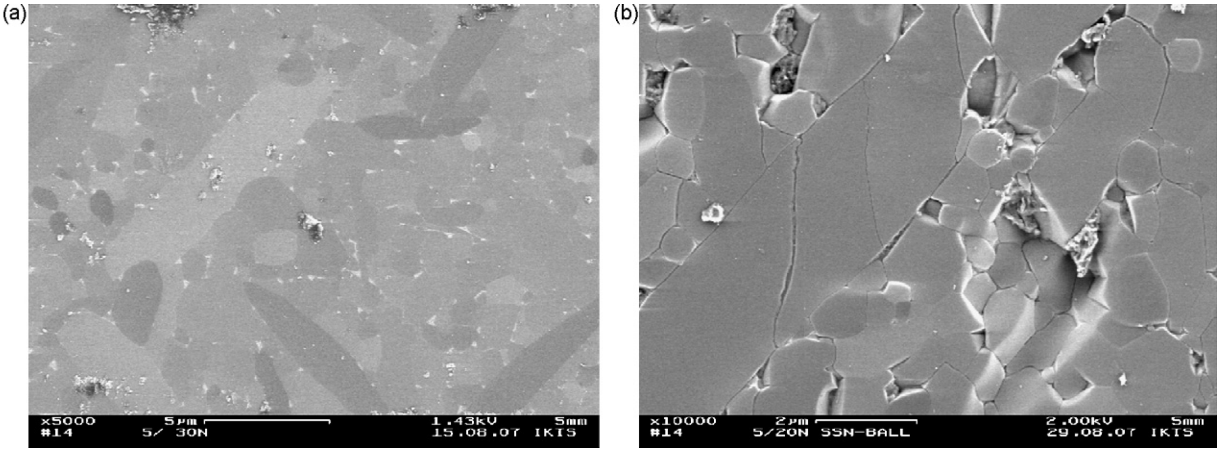

Fig. 2. FESEM micrographs of the worn surfaces of theY051-E2 material after fretting at a maximum Hertzian pressure of 1700 MPa against a 10 mm ball of (a) steel 100Cr6 and (b) silicon nitride.

the samples. A significant decrease of the friction coefficient (μ) was observed for all samples by increasing the load from 10 N to 30 N. Considering the variation of the μ values with sliding conditions, the specific wear rates also decreased for all samples with increasing normal load (Fig. 5). The development of surface layers by tribooxidation was accelerated by increasing Hertzian pressure. It should be noticed that samples containing single-phase α-SiAlON (N1251 and N1251-E2) showed worse wear rates than the other samples. This behaviour can be related to the grain morphology of the N1251 and N1251-E2 samples. Even though the Y1251-E2 sample also consists of almost pure α-SiAlON it has better wear behaviour than N1251 and N1251-E2.

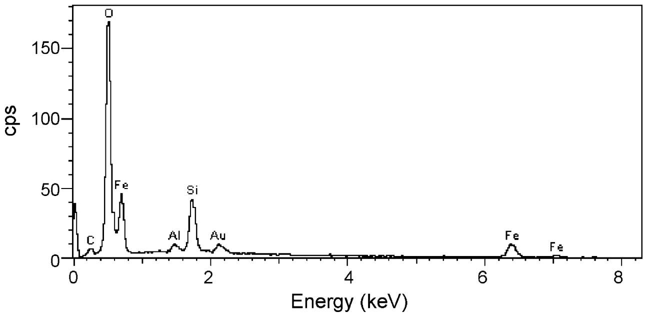

Fig. 3. EDX results of the layer on N1251 tested against the steel ball.

The α/β-SiAlON samples (Y051-E2 and N051-E2) have higher fracture toughness than pure α-SiAlON materials. Their grain size and aspect ratio are not significantly different (Fig. 6). But the wear resistance of α/β-SiAlON is better than that of the investigated pure α-SiAlON. Among the α/β-SiAlON materials, the Y-doped material Y051-E2 has the best wear resistance over the whole range of applied loads. The pure Y-α-SiAlON material (Y1251-E2) has only slightly higher friction coefficients (less than 10% increases) and at the highest applied load has smaller wear rate than all other materials.

This result indicates that the type of additive has influence on the material properties. According to literature the specific wear rate of Si_3N_4 materials, doped with different types of additives (Lu, Yb and Y), increased by increasing the cation size of the additive resulting in the change of the field strength.[28,29] Ionic field strength, defined as the ratio of valence to radius square of a cation. It can be a useful unifying parameter to interpret this situation. It is a measurement of the bonding

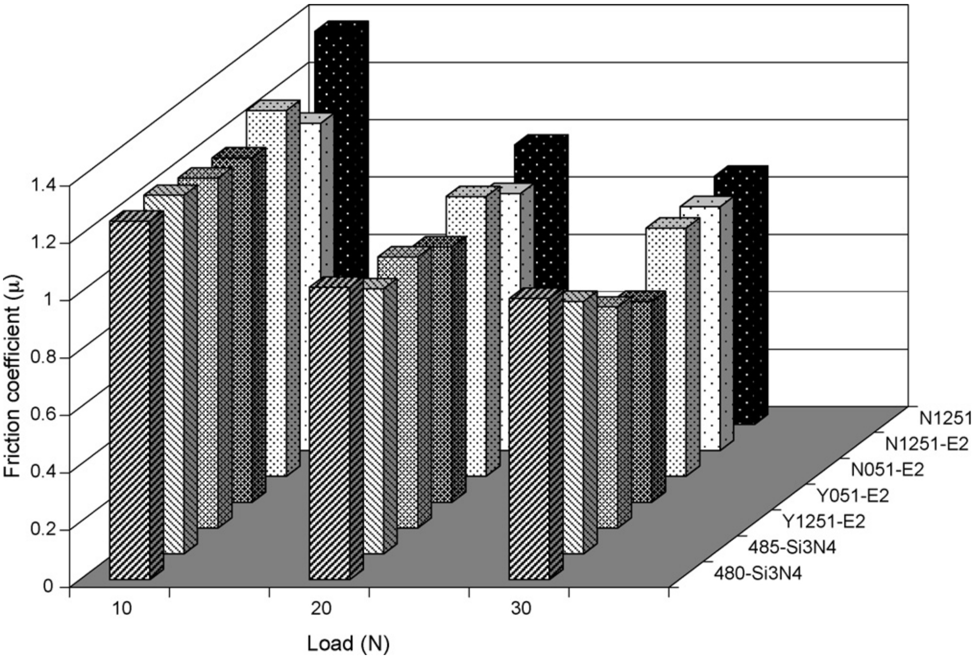

Fig. 4. Friction coefficient as a function of normal load and starting composition against a 10 mm steel ball.

interaction of the cation with neighbour ions. On the other hand, the structure of the thin films at the grain boundary is strongly different in the case of Y and Nd additives resulting in lower strength of the grain boundaries in Nd-doped β-SiAlON materials in comparison to the Y-doped materials. This lower grain boundary strength has a strong influence on the wear behaviour. Additionally, the effect of the amount of grain boundary phase is also directly related to the type of cation. The Y051 sample could not be densified by using the stochiometrical amount of additives (Table 1). Therefore, an additional amount of additive was used to increase the density and also to investigate the grain boundary phase effects on the wear properties. Although, both compositions Y051-E2 and N051-E2 contain 2 wt% excess amounts of additives, higher α-SiAlON content was observed in the Y051-E2 sample in comparison to the corresponding Nd-α-SiAlON (N051-

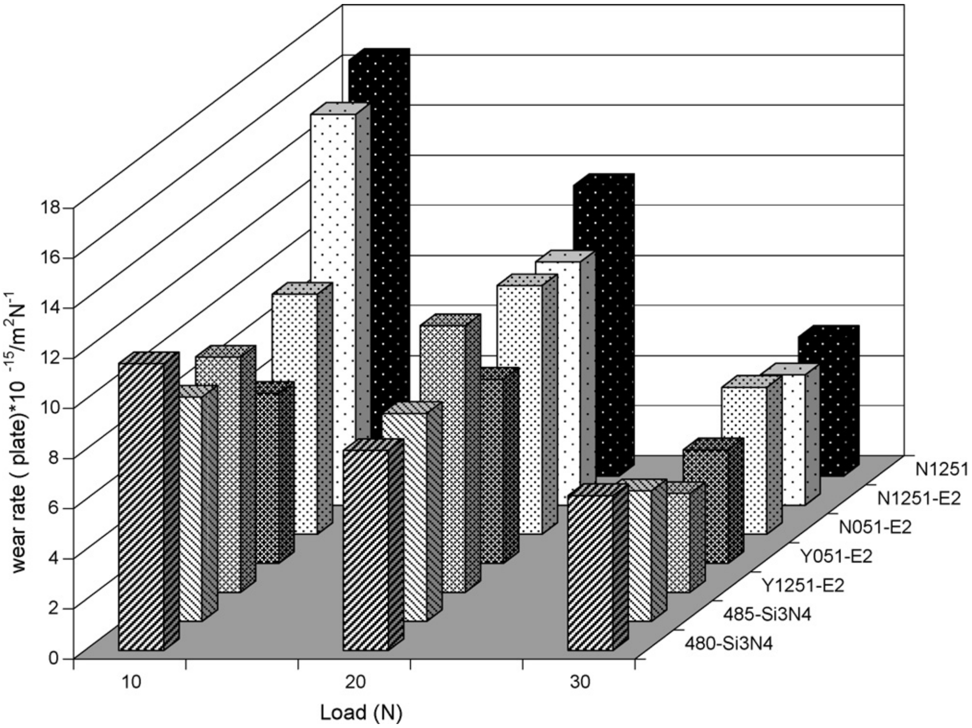

Fig. 5. Wear rate of materials as a function of normal load and starting composition against a 10 mm steel ball.

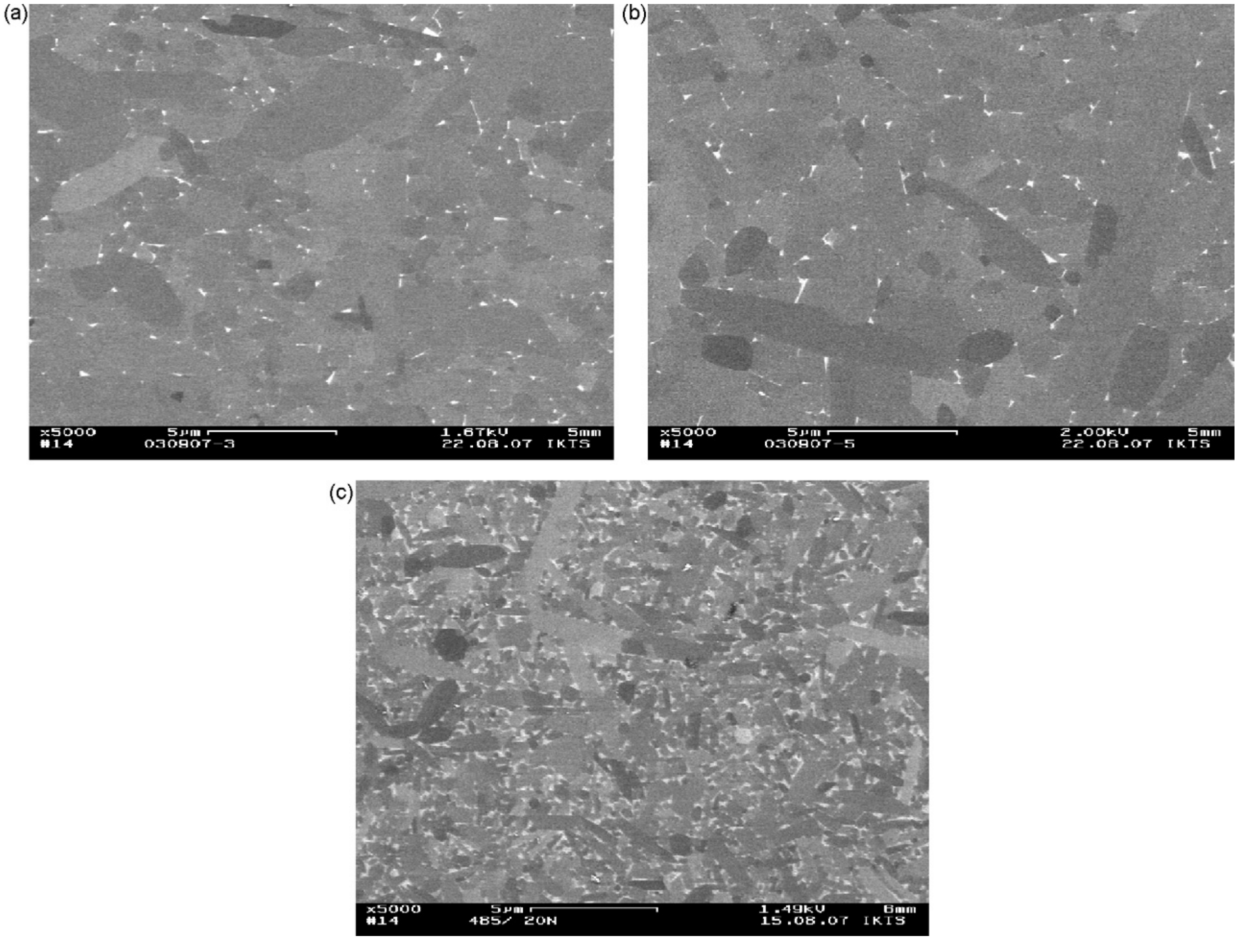

Fig. 6. Microstructure of the as-sintered materials. (a) N1251, (b) Y051-E2 and (c) 485 Si_3N_4.

E2) (Table 3). This indicates that a higher amount of rare earth is incorporated in the α-SiAlON lattice. Although, the same nominal amount of additives was used in both compositions, a higher amount of grain boundary phase exists for the Nd-containing material. This increasing amount of grain boundaries strongly deteriorates the wear properties of the materials.

Comparing the results with the reference β-Si_3N_4 materials, the wear rate of Y051-E2 is much lower than that of the reference β-Si_3N_4 material under all loads (Fig. 5). Even though β-Si_3N_4 samples have a finer microstructure with elongated grains and higher fracture toughness than the SiAlON materials (Fig. 6) their wear resistance is not as good as that of the Y-doped α/β-SiAlON Y051-E2. The micrographs of the worn

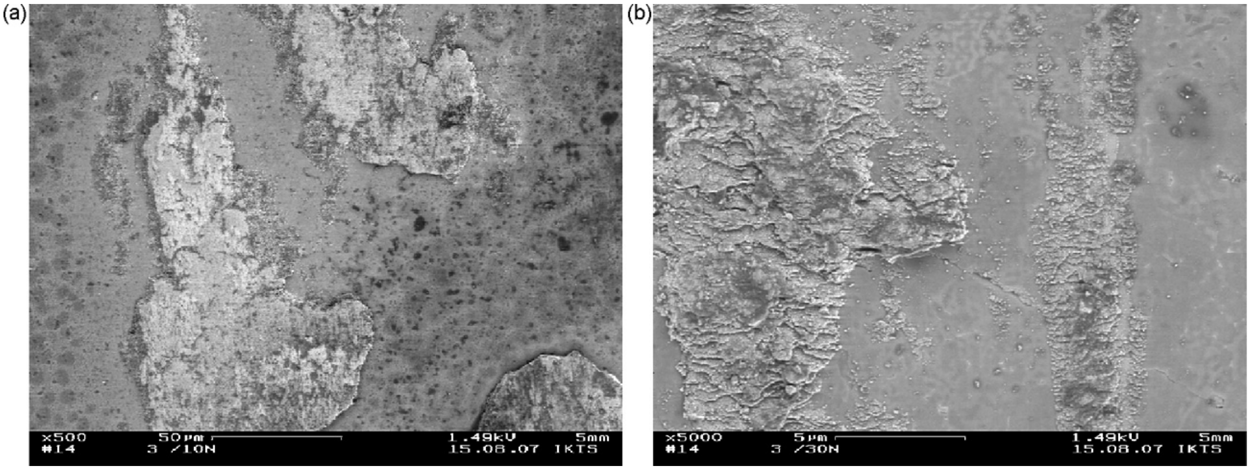

Fig. 7. Micrograph of the worn surface of the N1251 material after fretting against a 10 mm steel ball under the load of (a) 10 N and (b) 30 N.

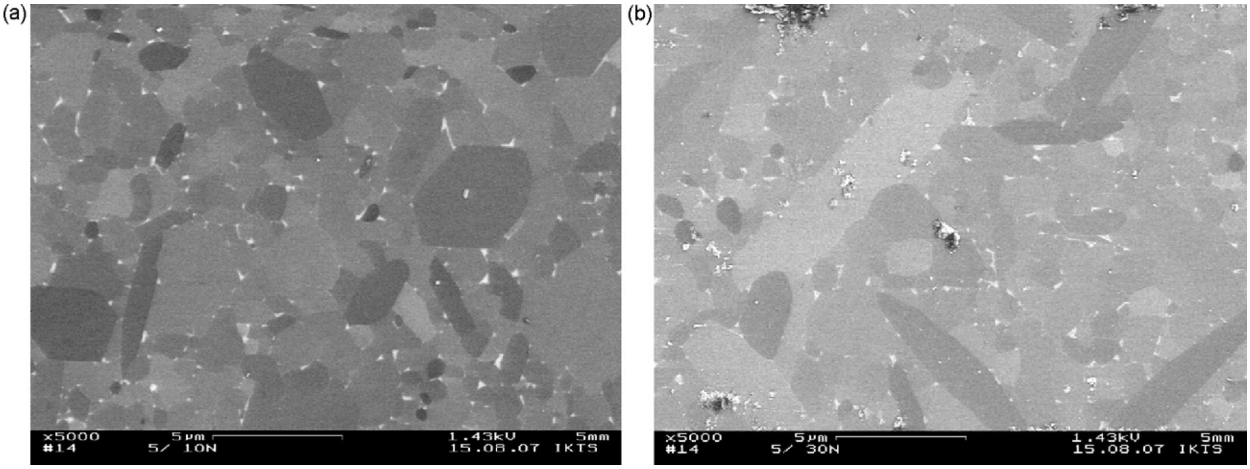

Fig. 8. Micrograph of the worn surface of the Y051-E2 material after fretting against a 10 mm steel ball under the load of (a) 10 N and (b) 30 N.

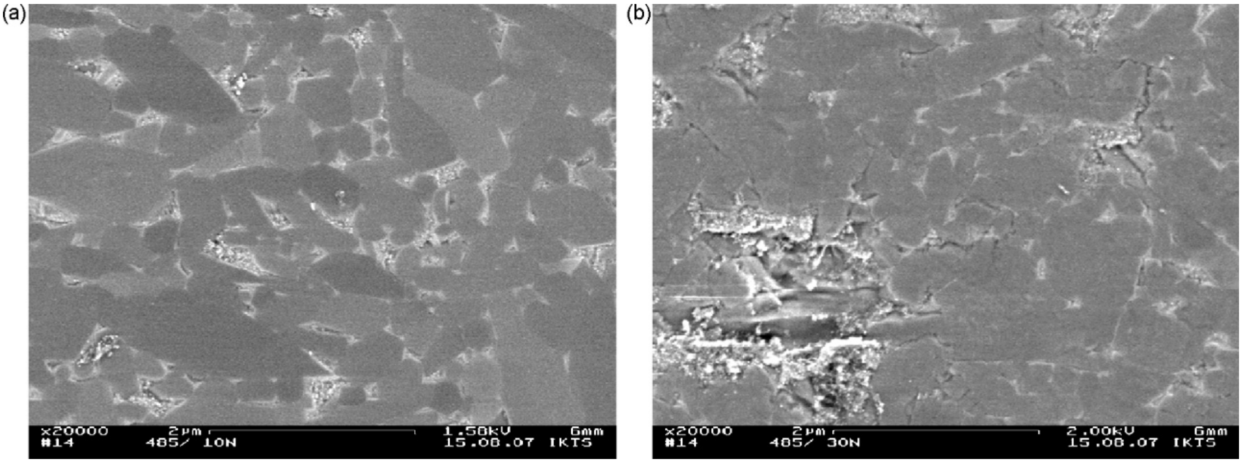

Fig. 9. Micrograph of the worn surface of the β-Si_3N_4 material 485 after fretting against a 10 mm steel ball under the load of (a) 10 N and (b) 30 N.

surfaces give the reason. While at the N1251 (Fig. 7) and Y051-E2 (Fig. 8) samples no removal of the grain boundary phase could be detected up to a load of 30 N, this process starts even at a load of 10 N in the 485 sample (Fig. 9). The different wear behaviour between SiAlON and β-Si_3N_4 materials is caused by the higher content of amorphous grain boundary phase in the β-Si_3N_4 materials in comparison to the α/β-SiAlON materials. The grain boundary strength in β-Si_3N_4 is lower than in SiAlON with the same rare-earth-sintering additive. Thus, the break out of grain boundary phase can start earlier in β-Si_3N_4 samples followed by cracking of the grains. This explains the differences between the β-Si_3N_4 and the Y-α/β-SiAlON materials. As stated above the kind of the rare earth has also a strong influence on the wear behaviour resulting in much higher wear rate of the Nd-α/β-SiAlON in comparison to the Y-α/β-SiAlONs of the same composition. This can be caused by the formed different amount of grain boundary phase (Nd-SiAlONs have higher amounts of grain boundary phase) and the different strength of the grain boundaries. Further investigations are necessary to understand this behaviour completely. Therefore, wear of the Nd-α/β-SiAlONs cannot be directly compared with the Y_2O_3 containing ß-Si_3N_4 materials used in this investigation.

4. Conclusion

The influence of Y- and Nd-doped single α- and α/β-SiAlON compositions on the wear properties was investigated during sliding contact under dry condition. The kind of rare-earth additive and the content of amorphous grain boundary phase were shown to have a significant effect on the wear behaviour. In particular, the materials sintered with Y led to a stronger grain boundary and superior wear resistance and mechanical properties. Additionally, the lowest friction value was observed for α/β-SiAlON compositions (Y051-E2), consisting of 81.10 wt% α-SiAlON and 18.90 wt% β-SiAlON. Considering the morphology of the worn surfaces, it can be reported that β-Si_3N_4 and SiAlON have a different wear behaviour which is related to the amount of grain boundary phase. Even though β-Si_3N_4 materials have a higher toughness and finer microstructure with a high aspect ratio as compared to Y051-E2 samples it was insufficient to tolerate the negative effect of the grain boundary strength on the wear behaviour of this material. These results showed that the wear properties of SiAlON ceramics can be tailored by selecting the starting composition and the type of additive.

The Nd-α/β-SiAlONs have a lower wear resistance than the Y-α/β-SiAlONs of the nominal same compositions. This can be caused by the differences in the amount and composition of the formed grain boundary phases. But further investigations are necessary to understand this behaviour.

Acknowledgements

This work is supported by a research grant from Deutscher Academischer Austausch Dienst (DAAD, Germany). One of the authors (S. Kurama) acknowledges financial support from DAAD. She would also like to thank the Fraunhofer Institute for Ceramic Technologies and Systems for assistance in the characterisation of materials.

References

1. Riley, F. L., Silicon nitride and related materials. *J. Am. Ceram. Soc.*, 2000, **83**, 245–265.
2. Hampshire, S., Park, H. K., Thompson, D. P. and Jack, K. H., α-SiAlON ceramics. *Nature*, 1978, **274**, 880–882.
3. Zhang, C., Sun, W. Y. and Yan, D. S., Optimizing mechanical properties and thermal stability of Ln-α-β-sialon by using duplex Ln elements (Dy and Sm). *J. Eur. Ceram. Soc.*, 1999, **19**, 33–39.
4. Ye, C., Liu, W., Chen, Y. and Ou, Z., Tribological behavior of Dy–sialon ceramics sliding against Si_3N_4 under lubrication of fluorine-containing oils. *Wear*, 2002, **253**, 579–584.
5. Skopp, A. and Woydt, M., Ceramic–ceramic composite materials with improved friction and wear properties. *Tribol. Int.*, 1992, **25**(1), 61–70.
6. Woydt, M., Materials-based concepts for an oil-free engine. In *New Direction in Tribology*, ed. I. M. Hutchings. Mechanical Engineering Publications, London, 1997, pp. 459–468.
7. Xu, J., Kato, K. and Hirayama, T., The transition of wear mode during the running-in process of silicon nitride sliding in water. *Wear*, 1997, **205**, 55–63.
8. Wong, H., Umehara, N. and Kato, K., The effect of surface roughness on friction of ceramics sliding in water. *Wear*, 1998, **218**, 237–243.
9. Childs, T. H. C. and Mimaroglu, A., Sliding friction and wear up to 600 °C of high speed steels and silicon nitrides for gas turbine bearings. *Wear*, 1993, **162–164**, 890–896.
10. Zhou, L., Fang, L., Wang, N. X. and Zhou, J. E., Unlubricated sliding wear mechanism of fine ceramic Si_3N_4 against high-chromium cast iron. *Tribol. Int.*, 1994, **27**(5), 349–357.
11. Wang, H., Kimura, Y. and Okada, K., Sliding friction and wear of ceramics at elevated temperatures up to 1000 °C. In *Proceedings of the Japan International Tribology Conference*, 1990, pp. 1389–1394.
12. Fang, L., Gao, Y., Zhou, L. and Li, P., Unlubricated sliding wear of ceramics against graphitized cast irons. *Wear*, 1994, **171**, 129–134.
13. Wani, M. F., Mukerji, J., Prakash, B. and Bandopadhyay, S., Friction and wear behaviour of hot-pressed SiAlON-steel ball tribopair under reciprocating sliding conditions. *Am. Ceram. Soc. Bull.*, 1993, **72**(9), 82–87.
14. Andersson, P. and Holmberg, K., Limitations on the use of ceramics in unlubricated sliding applications due to transfer layer formation. *Wear*, 1994, **175**, 1–8.
15. Gee, M. G. and Butterfield, D., The combined effect of speed and humidity on the wear and friction of silicon nitride. *Wear*, 1993, **162–164**, 234–245.
16. Gomes, J. R., Miranda, A. S., Silva, R. F. and Vieira, J. M., Tribological properties of AlN–CeO_2–Si_3N_4 cutting materials in unlubricated sliding against tool steel and cast iron. *Mater. Sci. Eng. A*, 1996, **209**, 277–286.
17. Gomes, J. R., Miranda, A. S., Silva, R. F. and Vieira, J. M., Tribo-oxidational effects on friction and wear behaviour of silicon nitride/tool steel and silicon nitride/gray cast iron contacts. *J. Am. Ceram. Soc.*, 1999, **82**(4), 953–960.
18. Gueroult, B. and Cherif, K. B., State of the art review on friction and wear mechanisms of ceramics. *J. Can. Ceram. Soc.*, 1994, **63**(2), 132–142.
19. Tomizawa, H. and Fisher, T. E., Friction and wear of silicon nitride at 150 °C to 800 °C. *ASLE Trans.*, 1985, **29**(4), 481–488.
20. Dong, X. and Jahanmir, S., Wear transition diagram for silicon nitride. *Wear*, 1993, **165**, 169–180.
21. Danyluk, S., McNallan, M. and Park, M. D. S., Friction and wear of silicon nitride exposed to moisture at high temperatures. In *Friction and wear of ceramics*, ed. S. Jahanmir. Marcel Dekker, New York, 1994, pp. 61–77.
22. Skopp, A., Woydt, M. and Habig, K. H., Tribological behavior of silicon nitride materials under unlubricated sliding between 22 °C and 1000 °C. *Wear*, 1995, **181–183**, 571–580.
23. Woydt, M., Ceramic–ceramic composites for dry sliding in closed tribosystems. *Am. Ceram. Soc. Bull.*, 1993, **72**(1), 66–67.
24. Sliney, H. E. and Dellacorte, C., The friction and wear of ceramic/ceramic and ceramic/metal combinations in sliding contact. *Lubric. Eng.*, 1994, **50**(7), 571–576.
25. Melandri, C., Gee, M. G., De Portu, G. and Guicciardi, S., High temperature friction and wear testing of silicon nitride ceramics. *Tribol. Int.*, 1995, **28**(6), 403–413.
26. Taut, T. and Bergmann, J., Rietveld-Analyse mit dem Programmsystem Refine ++, Handbuch der Version 1.1, 1998.
27. Amin, K. E., *Thoughness, Hardness and Wear Engineering Materials Handbook Ceramics and Glasses*, *4*. ASM International, 1991, p. 601.
28. Hyuga, H., Jones, M. I., Hirao, K. and Yamauchi, Y., Influence of rare-earth additives on wear properties of hot-pressed silicon nitride ceramics under dry sliding conditions. *J. Am. Ceram. Soc.*, 2004, **87**(9), 1683–1686.
29. Yu, J., Du, H., Shuba, R. and Chen, I. W., Dopant-dependent oxidation behaviour of α-SiAlON ceramics. *J. Mater. Sci.*, 2004, **39**, 4855–4860.